Electrical Power and Energy Systems 141 (2022) 108094

Contents lists available at ScienceDirect

International Journal of Electrical Power and Energy Systems

journal homepage: www.elsevier.com/locate/ijepes

A unit commitment model for optimal vehicle-to-grid operation in a power system

Ona Egbue [a,*], Charles Uko [b], Ali Aldubaisi [a], Enrico Santi [b]

[a] Department of Informatics and Engineering Systems, University of South Carolina Upstate, 800 University Way, Spartanburg, SC 29303, United States
[b] Department of Electrical Engineering, University of South Carolina, 301 Main Street, Columbia, SC 29208, United States

ARTICLE INFO

Keywords:
Economic dispatch
Plug-in electric vehicles
Power systems
Unit commitment
Vehicle-to-grid

ABSTRACT

Integrating plug-in electric vehicles (PEVs) into a smart grid can pose some challenges, particularly when a significant number of these vehicles are simultaneously charged and discharged. However, smart management of PEVs in a vehicle-to-grid (V2G) system can result in benefits to the grid such as load leveling, and cost reduction. This paper proposes a unit commitment model for a V2G system connected to a smart power grid. The model considers different penetration levels of PEVs and investigates the economic and technical effects of using PEVs to support the grid. The proposed methodology incorporates controlled charging and discharging as well as accounting for battery degradation in the unit commitment problem. The model is tested using an IEEE 24 bus network to determine the impact of high PEV penetration on generation cost. A comparison between a system without V2G and a system with V2G is presented to highlight the benefits of the proposed approach. The results show that the optimal scheduling of PEVs leads to reduction in generation cost and is effective in leveling the load profile through valley filling and peak load reduction.

1. Introduction

1.1. Aim and motivation

Rapid growth of energy demand has led to significant fossil fuel consumption and greenhouse gas emissions. To address alarming levels of greenhouse gas emissions, countries joined the Paris agreement to limit the global temperature increase to 2 degrees Celsius [1]. However, significant changes to major sources of emissions are needed to achieve this goal. In the United States, transportation and power generation account for roughly 55% of all greenhouse gas emissions [2]. Therefore, it is necessary to investigate sustainable options for power grid operation and transportation systems. One option is the use of plug-in electric vehicles (PEVs) as mobile energy storage units by intelligently scheduling their charging and discharging in a smart grid environment.

The projected growth of PEVs has the potential to introduce challenges to the operational stability of power systems [3]. These challenges can be mitigated by smart management of PEV energy demand and by using PEV batteries as back-up power supply to maintain grid stability [4–6]. Through bidirectional charging of PEVs, also known as vehicle-to-grid (V2G), PEV batteries can act as either storage or load. Other services that can be provided by bidirectional charging include peak shaving, reduction of power grid losses, power grid failure recovery, maximization of profit, minimization of emissions, valley filling, frequency, and voltage regulation [7]. Some drawbacks to bidirectional charging include high investment cost compared to traditional unidirectional stations, complicated hardware installation to support bidirectional power flow, battery degradation issues and social barriers [8,9]. Therefore, given the high replacement cost of PEV batteries, it is necessary to account for battery degradation when developing optimization models for V2G systems.

Despite many studies on V2G optimization, including studies that involve unit commitment (UC) with economic dispatch, the challenges posed by high penetration of PEVs have not been adequately addressed in the literature. In particular, there are gaps related to addressing the degradation of vehicle batteries and considering driving patterns when modeling V2G systems. To address the above deficiencies, this paper proposes a unit commitment model for the optimization of a V2G system connected to a smart power grid. The model considers different penetration levels of PEVs in a system and investigates the economic and technical effects of using PEVs to support the power grid. The model incorporates the travel behavior of individual drivers into V2G optimization and the unit commitment problem with economic dispatch. This paper makes the following contributions:

- Development of comprehensive modeling for battery degradation due to cycling from charging/discharging in a V2G system and

* Corresponding Author.
E-mail address: egbueo@uscupstate.edu (O. Egbue).

https://doi.org/10.1016/j.ijepes.2022.108094
Received 23 March 2021; Received in revised form 11 December 2021; Accepted 22 February 2022
Available online 25 April 2022

Nomenclature

Sets

B	Set of indices of bus connection matrix
I	Set of indices of plug-in electric vehicles
G	Set of indices of generating units
T	Set of indices of time periods
Ω	Set of indices of network branches

Indices

b	Column index of bus connection matrix
n	Row index of bus connection matrix
i	Index of plug-in electric vehicles
g	Index of generating units
t	Index of time periods

Binary Variables

$cend_{i,t}$	Ending status of a cycle for vehicle i at time period t
$cstart_{i,t}$	Starting status of a cycle for vehicle i at time period t
$c_{g,t}$	Charging status of vehicle i during time period t
$d_{g,t}$	Discharging status of vehicle i during time period t
$stable_{i,t}$	Idle status of vehicle i during time period t
$u_{g,t}$	ON/OFF status of generating unit g during time period t
$y_{g,t}$	Starting-up status of generating unit g during time period t
$z_{g,t}$	Shutting down status of generating unit g during time period t

Variables

$cycle_i$	Total number of cycles of vehicle i
$DOD_{i,t}$	Depth of discharge of vehicle i during time period t
F_g	Down time of generating unit g
L_g	Up time of generating unit g
P_g	Active power of generating unit g
P_{nb}	Active power between bus n and bus b
$Ptotal_t$	Total active power due to charging during time period t
$soc_{i,t}$	State of charge of vehicle i during time period t
$socE_{i,t}$	State of charge at the end of a cycle of vehicle i during time period t
$socS_{i,t}$	State of charge at the start of a cycle of vehicle i during time period t
$Shutdown_{g,t}$	Shutting-down cost of generating unit g during time period t
$Startup_{g,t}$	Starting-up cost of generating unit g during time period t

Parameters

a_g	Quadratic coefficient of fuel cost of generating unit g
b_g	Linear coefficient of fuel cost of generating unit g
ab_g	Constant coefficient of fuel cost of generating unit g
arr_i	Arrival time of vehicle i
CB_i	Battery cost of vehicle i
cap_i	Battery capacity of vehicle i
$Cdeg_{i,t}$	Degradation cost of vehicle i during time period
$costSD_g$	Shutting down cost of generating unit g
$costST_g$	Starting up cost of generating unit g
dep_i	Departure time of vehicle i
$DT_{g,0}$	Time that unit g has been down before the planning horizon
$Fcost_{g,t}$	Fuel cost of generating unit g during time period t
$initial\_soc_i$	Initial state of charge of vehicle i
k	Slope of the cost of battery degradation equation
$minDT_g$	Minimum down time for generating unit g
$minUT_g$	Minimum up time for generating unit g
$Msoc_i$	Minimum state of charge of vehicle i
η_1, η_2	Charging and discharging efficiencies
$Pmax_g$	Maximum operating power limit for generating unit g
$Pmin_g$	Minimum operating power limit for generating unit g
Pr_{nb}	Maximum power flow limit between bus n and bus b
$RampDown_g$	Ramp down power limit for generating unit g
$RampUp_g$	Ramp up power limit for generating unit g
SD_g	Shutdown power limit for generating unit g
SU_g	Startup power limit for generating unit g
$u_{g,0}$	Initial operating status of generating unit g
$UT_{g,0}$	Time that unit g has been up before the planning horizon
V_n	Voltage magnitude at the bus
δ_b	Voltage angle for bus b
δ_n	Voltage angle for bus n
x_{nb}	Reactance of the branch connecting bus n and bus b

computation of the associated costs. This is typically neglected in UC and V2G optimization studies leading to inaccurate cost models.

- Incorporation of driving and charging/discharging behavior patterns in V2G optimization. This has been shown to be highly correlated with system flexibility. However, it is often overlooked.

1.2. Literature review

Unit commitment (UC) is a key optimization task in power systems management to determine the optimal set of binary on/off status of the available generating units that minimizes the total operation cost while satisfying certain constraints over a short-term horizon. Traditional UC problems are usually formulated as a mixed-integer non-linear program (MINLP) subject to economic constraints [10]. UC problems have been studied extensively in the literature and numerous models have been proposed to formulate and solve the UC problem for conventional power systems [11–13].

Several studies have proposed security constrained UC models for bidirectional charging in smart power systems which is essential for the independent system operator to make operational decisions [14–17]. In security constrained problems, network characteristics and limits are considered to ensure a physically feasible solution to the UC Problem [18]. Hosseini Imani et al. [19] proposed a security-constrained UC model considering cases with V2G and without V2G. The model was applied to IEEE 6 and 33 bus systems and showed significant reduction in the hourly operation cost when considering V2G. Sadeghian and Wang [20] examined a power system that utilized combined heat and power (CHP) units and PEVs in addition to conventional thermal generating units to reduce the generation cost of the power system. Their simulation model has 50,000 PEVs aggregated from various smart parking lots in the system. Although V2G was considered to solve the unit commitment problem, all vehicles were assumed to have the same battery parameters. Yang et al. [21] introduced a binary symmetric based hybrid meta-heuristic method for solving a mixed-integer unit commitment problem with significant penetration of PEVs. The study investigated a 10-unit power system with 50,000 plug-in electric vehicles and considered unidirectional and bidirectional operation modes. The results show that V2G was effective in reducing the cost of operation. Azari et al. [22] studied the effect of V2G on the operation cost and locational marginal price (LMP) using IEEE 6 bus system. The ability of the electric vehicle load demand to be delayed to a later period was able to prevent the use of expensive units to generate power thus reducing the line congestion and decreasing the LMP.

PEVs can also play a significant role in mitigating the risk of

renewable energy volatility on grid operations. Cao and Zhao [23] introduced a multi-objective security-constrained UC model that considers wind power and V2G. Their simulation was conducted on the IEEE 24-bus system, and their model was effective in achieving peak load shifting, reducing energy cost, and reducing the PEV owner's electric charges. In some studies, [24,25], Monte Carlo simulation was used to account for the uncertain outputs of renewable sources, and meta-heuristic algorithms were used to solve the UC problem. The findings indicate that the use of PEVs led to a decrease in the total cost of power generation in the system while reducing the impact of the uncertainty of renewable sources. Yang et al. [26] proposed a multi-zone sampling method to generate stochastic wind and solar generation profiles and solved the UC problem with and without PEVs. Although the intelligent scheduling of PEVs saved only 0.05 $/MW on average, PEVs provided a relief to the uncertainty of the renewable energy resources. Vasiyullah and Bharathidasan [27] proposed two-stage optimization model with improved pre-prepared power demand to solve the UC problem for a system with ten thermal units, renewable energy sources and PEVs. In these studies, V2G has shown an average reduction in total cost of generation ranging from 0.9% to 1.5% in comparison to uncontrolled charging, but the cost of battery degradation was not considered.

It is important to study PEV driving behavior because it has a significant impact on the distribution network and the utilization of the charging infrastructure [28]. Uko et al. [29] proposed an economic dispatch model considering the arrival time distribution of PEVs at different buses and the cost of battery degradation to reduce the power cost. Shamshirband et al. [30] considered driving behavior of PEVs with different battery capacities and different load profiles. Although UC was not considered in these studies, V2G was effective for frequency control. To provide more accurate results on the impact of PEVs on the power system, studies have incorporated driving information in the UC problem. Deng et al. [31] presented a dispatching strategy for balancing the load demand considering dynamic driving and charging behaviors. Pan et al. [32] considered the traveling behavior of PEVs on the security constrained UC problem to achieve the best schedules for the V2G dispatch. Ahrabi et al. [33] used Monte Carlo simulation to address the uncertainty of driving behaviors. Ahmadi et al. [34] presented a multi-objective security-constrained UC optimization model with deterministic driving profiles. These UC models were successful in accommodating the uncertainty of renewable energy sources and reducing the power cost when compared to uncontrolled charging and discharging.

The rest of the paper is organized as follows: the mathematical formulation of the proposed problem is presented in Section 2; Section 3 presents numerical results of UC problem scenarios of a smart grid with unidirectional (charging only) and bidirectional (V2G) PEV scheduling. Three PEV penetration levels for each scheduling method in addition to the base UC problem with no PEVs are studied in this section. The total cost of power generation, battery degradation cost and the energy profiles of the generating units are analyzed; Section 4 concludes the paper and proposes some directions for future work.

2. Methodology

This paper considers a UC problem with different PEV penetration levels to investigate the economic impact of using PEVs to support the smart grid and the effect on leveling power system generation. The proposed model considers the PEV drivers' driving behavior and battery degradation simultaneously [35]. In addition, this paper considers vehicle physical properties in modeling the problem. For ease of modeling, a discrete-time system is used to approximate the continuous-time used for the simulation. A total of 48 intervals of 1 h each is used for the simulation of a planning horizon of 2 days. All vehicle arrivals and most departure occur during the first day. However, a second day is added to capture the departure time of vehicles that arrive late on the first day and cannot complete charging by the end of the first day. In this paper, information such as the arrival and departure time of the PEVs as well as the vehicle characteristics are assumed to be known ahead of time. Travel patterns, arrival and departure times as well as attributes such as travel speed, average commute distance to several destinations, and dwell time at each destination are all based on the National Household Travel Survey (NHTS) historical travel data [36]. Information on the vehicles' physical properties is obtained from the U.S. Department of Energy [37].

2.1. Mathematical formulation of the unit commitment problem

The optimization problem is tested using a modified IEEE 24 bus system adapted from [38] as shown in Fig. 1. The system is composed of 24 buses, with 34 power lines and 10 generators. The PEV charging stations have been randomly assigned to buses 1, 3, 15, 19 and 24 for this study.

The following assumptions are made for the formulation of the unit commitment problem.

1. The three-phase system is balanced, and voltage regulators, transformers and switches are not considered.
2. Charging stations are in constant communication with each other and are centrally controlled.
3. Each PEV departure time, desired minimum state of charge (SOC) and target SOC at departure are known at time 0.
4. PEV discharging energy represents a proportion of PEV charging energy in the V2G cases
5. Charging units are equipped with smart metering technology and can directly access PEVs' SOC. This is necessary to obtain the dynamic SOC of PEVs.
6. The central controller is in constant communication with the smart grid.
7. PEVs and loads are evenly distributed between buses and phases.
8. Power flow in the bus system is based on a DC power flow framework. This assumption is made because DC power flow is absolutely convergent which reduces the computational complexity.
9. The angle of the slack bus and the susceptance between buses and the ground are zero.
10. The voltage profile is flat for all buses and the voltage angle difference between adjacent nodes is small.
11. Reactive power and transmission losses are not considered.

2.1.1. Objective function

Generally, fuel costs of thermal generators in an economic dispatch problem are described as a quadratic function [39] shown in equation (1).

$$\text{Fcost} = \sum_{g=1}^{G} a_g P_g^2 + b_g P_g + ab_g \tag{1}$$

where G is the number of generating units; a_g, b_g, and ab_g are the cost coefficients of the g^{th} generating unit, and P_g is the active output power of the generating unit. The objective function of the proposed UC problem is the summation of fuel costs, *Fcost*, startup costs, *costST* and shutdown costs, *costSD* of thermal units, and the cost of battery degradation, $Cdeg_{i,t}$ for PEV $i(i = 1, 2, 3, \cdots I)$ during time period $t(t = 1, 2, 3, \cdots T)$ as shown in Equation (2) below.

$$\sum_{g=1}^{G}\sum_{t=1}^{T}(u_{g,t}{*}Fcost_{g,t}) + (y_{g,t}{*}\,\text{costST}_g) + (z_{g,t}{*}\,\text{costSD}_g) + \sum_{i}^{I}\sum_{t}^{T}(c_{i,t} + d_{i,t}){*}Cdeg_{i,t} \tag{2}$$

where $u_{g,t}, y_{g,t}, z_{g,t}, c_{i,t}$ and $d_{i,t}$ are binary variables indicating generator status, starting up, shutting down, charging, and discharging, respectively. The objective function is subject to the following constraints:

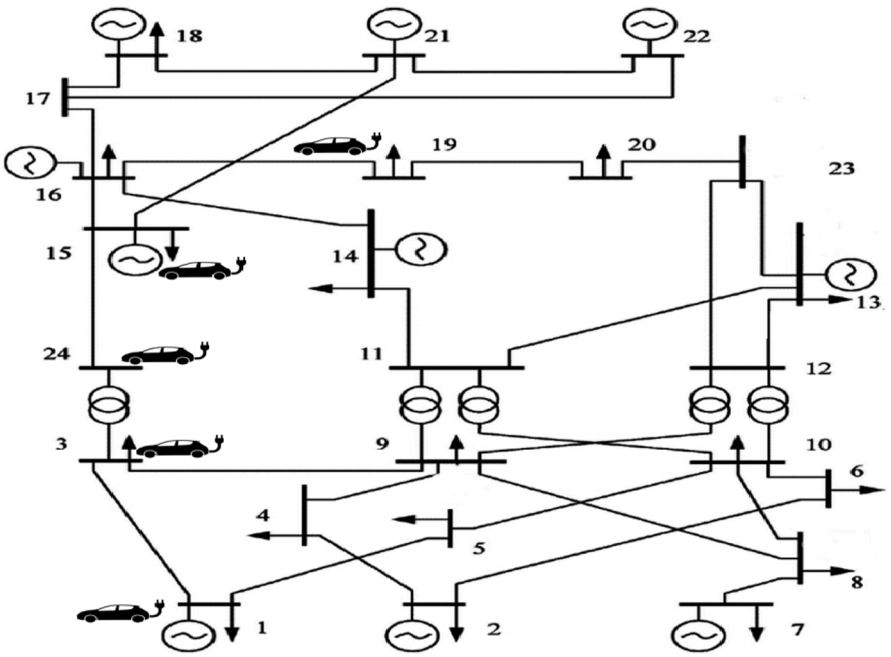

Fig. 1. Modified IEEE 24 Bus system.

2.1.2. Charging and discharging constraints

Equation (3) is a constraint specifying that charging and discharging can only take place when the vehicle is available in the parking lot.

$$c_{i,t} + d_{i,t} = 0 \ \forall \ arr_i \leq t \leq dep_i \tag{3}$$

where arr_i and dep_i are the arrival and departure time of vehicle i, respectively. The constraint in equation (4) prevents charging and discharging from occurring at the same time.

$$c_{i,t} + d_{i,t} \leq 1 \tag{4}$$

Equation (5) caps the upper limit of the SOC to 90% of the battery capacity to limit battery degradation from overcharging. Based on equation (6), a vehicle battery cannot be discharged if the SOC is below the minimum required SOC.

$$soc_{i,t} \leq 0.9 * cap_i \tag{5}$$

$$d_{i,t} = 0 \ \forall \ Msoc_i \geq soc_{i,t} \tag{6}$$

where cap_i and $Msoc_i$ are the battery capacity and the minimum desired SOC for vehicle i, respectively. Equation (7) shows the relationship between SOC in the current period and SOC in the preceding period based on whether charging or discharging occurs.

$$soc_{i,t} = soc_{i,t-1} + (c_{i,t} * \eta_1) - (d_{i,t} * \eta_2) \tag{7}$$

where η_1 and η_2 are the charging and discharging efficiencies, respectively. The total power due to charging in each period is described in Equation (8).

$$Ptotal_t = \sum_{i=1}^{I} c_{i,t} \tag{8}$$

2.1.3. Power generating unit constraints

The total active power is determined by total non PEV load demand and PEV load demand and supply. The formulation for this relationship is expressed in Equations 9–26 where the load balance at the bus with PEVs is accounted for by the operating power of generator P_g, non-PEV loads and PEV loads. Because of the quadratic nature of the economic dispatch problem, the model becomes a challenging non-linear optimization problem. The fuel cost function is linearized by dividing the cost function into piece-wise linear segments. The fuel curve between the intervals *Pmin* and *Pmax* is divided into equally sized linear intervals, which, when aggregated, are an estimate of the quadratic cost function. The precision of this linearized form can be increased by increasing the number of intervals between *Pmin* and *Pmax* [40]. Equations (9) and (10) are constraints that ensure that the generating unit operates within the lower and upper operating limits.

$$Pmin_g \leq P_{g,t} \tag{9}$$

$$P_{g,t} \leq Pmax_g \tag{10}$$

Equations (11) and (12) ensure that generation units cannot start up and shut down at the same time. Where $u_{g,t}$ is a binary variable representing on and off state at 1 and 0, respectively. $y_{g,t}$ is a binary variable representing the start-up state and $z_{g,t}$ is a binary variable representing the shut-down state.

$$y_{g,t} - z_{g,t} = u_{g,t} - u_{g,t-1} \tag{11}$$

$$y_{g,t} + z_{g,t} \leq 1 \tag{12}$$

Equations (13) and (14) calculate the cost of starting up and shutting down the generator. Where $y_{g,t}$ and $z_{g,t}$ are binary variables for starting up and shutting down, respectively.

$$Startup_{g,t} = y_{g,t} * costST_g \tag{13}$$

$$Shutdown_{g,t} = z_{g,t} * costSD_g \tag{14}$$

Equations (15) to (22) impose availability limits on the generating unit to satisfy the minimum up time and down time of the generating units. Where L_g and F_g are the number of periods unit g must stay up and down respectively. Initial conditions are assigned to all units to indicate the initial operating status $U_{g,0}$, and the time that unit g has been up $UT_{g,0}$ or down $DT_{g,0}$ before the beginning of the planning horizon. Minimum required up and down times, *minUT* and *minDT* ensure that the minimum up time and down time have been reached. If the unit is on at time $(t-1)$ and turned off at time t, then the generated power at time $(t-1)$ should be less than the shutdown limit,SD_g.

$$\sum_{t=1}^{L_g} 1 - u_{g,t} = 0 \ \forall \ g \in G, \ \forall \ t \in 1, \ldots\ldots L_g \tag{15}$$

$$L_g = min\{T, (minUT_g - UT_{g,0})^*U_{g,0}\} \quad (16)$$

$$\sum_{t=1}^{L_g} u_{g,t} - y_{g,t} \geq 0 \quad (17)$$

$$\sum_{t=1}^{T} u_{g,t} \geq y_{g,t}^*minUT_g \ \forall\ g \in G,\ \forall\ t \in 1, \cdots\cdots T - minUT_g + 2 \quad (18)$$

$$\sum_{t=1}^{F_g} u_{g,t} = 0 \ \forall\ g \in G,\ \forall\ t \in 1, \cdots\cdots F_g \quad (19)$$

$$F_g = min\{T, (minDT_g - DT_{g,0})^*(1 - U_{g,0})\} \quad (20)$$

$$\sum_{t=1}^{F_g} 1 - u_{g,t} - z_{g,t} \geq 0 \quad (21)$$

$$\sum_{t=1}^{T} 1 - u_{g,t} \geq z_{g,t}^*minDT_g \ \forall\ g \in G,\ \forall\ t \in 1, \cdots\cdots T - minDT_g + 2 \quad (22)$$

Equation (23) ensures that a power drop from one period to the next does not exceed the ramp down limit, $RampDown_g$. In case of shutdown in the next hour (t + 1), constraint (24) ensures power does not exceed the shutdown limit SD_g.

$$P_{g,t-1} - P_{g,t} \leq u_{g,t}^*RampDown_g + z_{g,t}^*SD_g \quad (23)$$

$$P_{g,t} \leq (u_{g,t} - z_{g,t+1})^*Pmax_g + z_{g,t+1}^*SD_g \quad (24)$$

If the unit is turned off in the previous hour and then turned on at time t, then $P_{g,t}$ cannot be more than start up limit, SU_g. Equation (25) specifies that an increase in power from one period to the other does not exceed the ramp up limit, $RampUp_g$.

$$P_{g,t} \leq P_{g,t-1} + (u_{g,t-1}^*RampUp_g) + y_{g,t}^*SU_g \quad (25)$$

Equation (26) makes sure that the total power flow between the buses is balanced in relation to both the PEV demand and supply, and the non-PEV loads, $Load_{b,t}$.

$$\sum_{b=1}^{B} P_{g,t} - Load_{b,t} - TotalEVDemand_{b,t} + TotalEVSupply_{b,t} = \sum_{nb} P_{nb} \quad (26)$$

The scheduling of the PEVs during the optimization process occurs at the buses where the PEVs are located. In this paper, DC power flow is used as a linearization of AC power flow, therefore only active power is considered. The power flow at node n for every branch in Ω is specified in equation (27).

$$P_n = V_n \sum_{b=1}^{B} V_n(G_{nb}^*cos(\delta_{nb}) + B_{nb}^*sin(\delta_{nb})) \quad (27)$$

Reactive power and transmission losses are neglected which means line resistances are negligible. Therefore, the imaginary part G of equation (27) is assumed to be zero. The susceptance between buses and the ground is assumed to be zero and the imaginary part of the bus admittance matrix, B_{nb} is approximated by the reciprocal of the reactance (i.e., $\frac{-1}{x_{nb}}$). Furthermore, it is assumed that voltage magnitude V_n is 1.0 p.u. for all buses and the voltage angle differences between adjacent nodes are small (i.e., $sin(\delta_{nb}) \approx \delta_n - \delta_b$). As a result, the active power, P_{nb} between bus n and bus b can be approximated by equation (28).

$$P_{nb} = \frac{\delta_n - \delta_b}{x_{nb}}, nb \in \Omega \quad (28)$$

$$P_{nb} \leq Pr_{nb}, nb \in \Omega \quad (29)$$

where δ_n and δ_b are the voltage angles for buses b and n respectively. x_{nb} *is the* reactance of the branch connecting bus b to n. Equation (29) sets the upper power flow limit Pr_{nb} of the branch connecting bus b to n. The angle of the slack bus in this case is assumed to be zero.

2.1.4. Battery degradation constraints

Battery degradation occurs due to calendar aging and cycling aging. Calendar aging degrades the battery over time and is caused mainly by temperature while cycling aging is caused by charging and discharging cycles [41]. Since cycling aging occurs during the V2G process due to repeated deep cycling of the battery [42], this paper focuses on cycling aging and does not consider calendar aging. A cycle occurs when a battery discharges to a certain depth of discharge and then charges back to the initial SOC at which the discharging began. To account for the cost of battery degradation due to cycling, a linear model by Ortega-Vazquez [43] has been adopted.

Let $c_{i,t}$, $d_{i,t}$ and $stable_{i,t}$ be variables that indicate when there is an increase, a decrease, or no change in the SOC, respectively. Binary variables *cstart* and *cend* are also introduced to represent the start and end of a cycle respectively. Then equations 30–37 below are used to define and account for cycles.

$$soc_{i,t} - soc_{i,t-1} > 0 \Leftrightarrow c_{i,t} = 1 \ \forall\ i \quad (30)$$

$$soc_{i,t} - soc_{i,t-1} < 0 \Leftrightarrow d_{i,t} = 1 \ \forall\ i \quad (31)$$

$$soc_{i,t} - soc_{i,t-1} = 0 \Leftrightarrow stable_{i,t} = 1 \ \forall\ i \quad (32)$$

$$c_{i,t} + d_{i,t} + stable_{i,t} = 1 \ \forall\ i \quad (33)$$

$$d_{i,t} - d_{i,t+1} + cstart_{i,t} - cend_{i,t} = 0 \ \forall\ i, t > 1 \quad (34)$$

$$cstart_{i,1} = d_{i,1} \ \forall\ i \quad (35)$$

$$\sum_t cstart_{i,t} = \sum_t cend_{i,t} \quad (36)$$

$$cycle_i = \sum_t cend_{i,t} \quad (37)$$

In equations 38–41, an auxiliary variable $socS_{i,t}$ is introduced to retain the value of the SOC when a cycle starts and $socE_{i,t}$ retains the value of the SOC at the end of the cycle. Equation (38) sets the starting SOC to the initial SOC for a cycle that starts at the beginning of the planning horizon; otherwise, the starting SOC is set to the SOC of the battery at the beginning of the cycle according to equation (39).

$$socS_{i,t} = initial\_soc_i \Leftrightarrow cstart_{i,1} = 1 \ \forall\ i \quad (38)$$

$$socS_{i,t} = soc_{i,t} \Leftrightarrow cstart_{i,t} = 1 \ \forall\ i, t > 1 \quad (39)$$

$$socS_{i,1} = initial\_soc_i \Leftrightarrow d_{i,t} = 1 \ \forall\ i \quad (40)$$

$$socS_{i,t} = soc_{i,t-1} \Leftrightarrow d_{i,t} = 1 \ \forall\ i \quad (41)$$

$$socE_{i,t} = soc_{i,t} \Leftrightarrow cend_{i,t} = 1 \ \forall\ i, t \quad (42)$$

Equation (40) ensures that the starting SOC for a cycle is set to the initial SOC at the start of the cycle if discharging happens at first time interval. If discharging begins at time $t(t > 1)$, the starting SOC of the cycle is set to the SOC of the battery at the end of the previous time interval according to equation (41). Equation (42) determines the ending SOC at the end of the cycle *cend*. DOD is calculated by subtracting the SOC at the end of the cycle, $socE_{i,t}$ from the SOC at the beginning of the cycle $socS_{i,t}$, as shown in equation (43).

$$DOD_{i,t} = socS_{i,t} - socE_{i,t} \Leftrightarrow cend_{i,t} = 1 \ \forall\ i, t \quad (43)$$

Lastly, Equation (44) calculates the battery degradation cost. Where k represents the slope of the linear approximation of the battery life as a function of the cycles. cap_i is the battery capacity, CB_i is the battery cost, and $DOD_{i,t}$ is the depth of discharge. The cost of batteries used for the simulation is obtained from a study conducted by the U.S. International Trade Commission [44].

$$Cdeg_{i,t} = \left|\frac{k}{100}\right|^*2^*\frac{DOD_{i,t}}{cap_i}^*CB_i \quad (44)$$

3. Results and discussion

In this paper, two charging scenarios for PEVs namely unidirectional (charging only) and bidirectional (V2G), are considered and integrated into the UC problem. The proposed model is demonstrated using an IEEE 24-bus system with 10 generators, and 34 transmission lines. Seven different cases are considered for this test system. The first case is a base case where PEVs are not deployed. The results of the base case are used as a benchmark to evaluate the effect of PEVs in the other cases considered. In cases 2 to 4, three levels of PEVs penetration are simulated in a system where unidirectional charging is implemented. This means that on arrival at a charging station, the vehicles immediately begin charging at the maximum charging rate of 6.6 kWh until their desired SOC. In cases 5 to 7, the same levels of PEVs penetration considered in cases 2 to 4 are examined with V2G implemented and incorporating controlled scheduling of charging and discharging as well as battery degradation costs. It is assumed that total PEV discharged energy is at least a third of PEV charged energy. To demonstrate the impact of large-scale deployment of PEVs, three penetration levels of 10,000, 100,000 and 1,000,000 PEVs are considered.

The travel pattern of 20,000 vehicles from the NHTS trips dataset is analyzed, and the arrival time distribution for the vehicles is fitted non-parametrically. The authors assume the PEV parking to include work, school, daycare, shopping, as well as religious and leisure activities. Fig. 2 shows the arrival time distribution of vehicles for the locations mentioned above.

The dwell time, which is the time the vehicle spends at the parking lot, is also obtained from the NHTS trips dataset. The time for vehicles' departure is estimated as the sum of the arrival time and the dwell time. Battery data including initial SOC, minimum required SOC, target SOC, battery capacity and battery cost are generated based on the sales distribution of PEVs in the market obtained from [45]. Finally, PEVs are randomly assigned to the selected buses. Network technical characteristics, lines capacity, generation costs and the base UC model are obtained from Soroudi [40]. This includes reactance and lines capacity for the IEEE 24-bus network as shown in Table 1.

The mathematical model was implemented in the General Algebraic Modeling System software (GAMS) as a mixed-integer linear programming model (MILP) considering a 48-hour scheduling horizon with a time step of one hour. CPLEX solver was utilized to solve the UC problem using a PC with i7-7700K CPU and 16 GB RAM. Default options were used for branch and cut method [46] with 0.5% optimality tolerance. The branch-and-cut method generates a search tree of linear subproblems consisting of lower and upper bounds for the committed thermal units at each hour. The tree is initialized to contain the root subproblem which represents the entire UC problem without integrality constraints. Cuts are generated for the root subproblem to find an incumbent solution that satisfies all integrality constraints. Cuts represents constraints that are added to reduce the solution domain. The node is solved again after adding cuts until no more constraints are violated. If any constraint is violated during this procedure, the node becomes infeasible, and the algorithm removes it from the tree. If the node is feasible and the solution is better than the incumbent solution, the node solution becomes the new incumbent. Otherwise, the algorithm generates two new nodes representing a new branch. Each feasible node solution is compared to the incumbent solution and this procedure continues until the percentage difference between the two solutions is less than the predefined optimality tolerance.

Table 1
Reactance and power flow limits for IEEE 24-bus network [40].

From	To	x_{nb} (p.u)	Pr_{nb} (MVA)	From	To	x_{nb} (p.u)	Pr_{nb} (MVA)
1	2	0.0139	500	11	13	0.0476	500
1	3	0.2112	500	11	14	0.0418	500
1	5	0.0845	500	12	13	0.0476	500
2	4	0.1267	500	12	23	0.0966	500
2	6	0.192	500	13	23	0.0865	500
3	9	0.119	500	14	16	0.0389	500
3	24	0.0839	500	15	16	0.0173	500
4	9	0.1037	500	15	21	0.0245	1000
5	10	0.0883	575	15	24	0.0519	500
6	10	0.0605	575	16	17	0.0259	500
7	8	0.0614	575	16	19	0.0231	500
8	9	0.1651	575	17	18	0.0144	500
8	10	0.1651	575	17	22	0.1053	500
9	11	0.0839	400	18	21	0.01295	1000
9	12	0.0839	400	19	2	0.0198	1000
10	11	0.0839	400	20	23	0.0108	1000
10	12	0.0839	400	21	22	0.0678	500

3.1. Case 1- base case without PEVs

To evaluate the effect of aggregated PEVs on the UC problem, a base case which does not include PEVs is considered. Fig. 3 shows the hourly energy profile for each generating unit.

In this case, since PEVs are not considered in the test system, the model minimizes the generation cost while meeting the load demand. All generators start with their initial power generation values at the

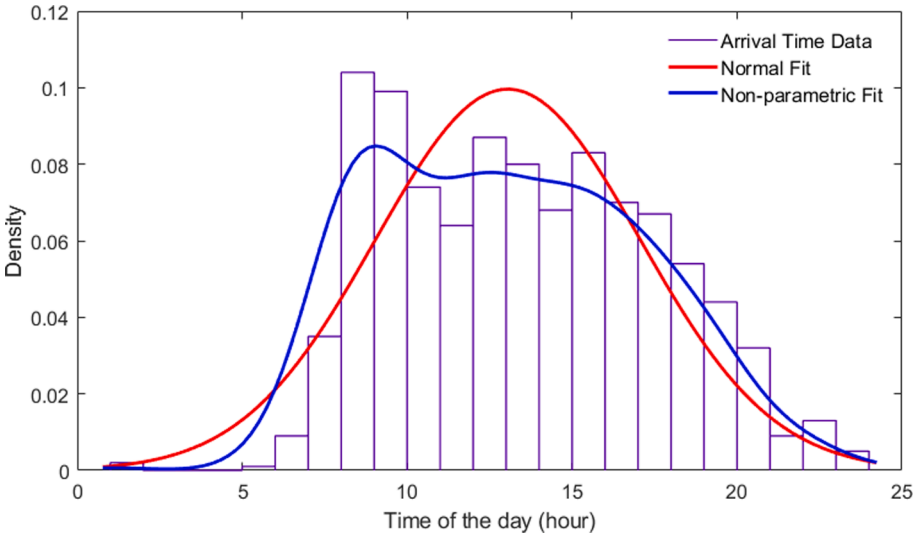

Fig. 2. Arrival distribution for vehicles.

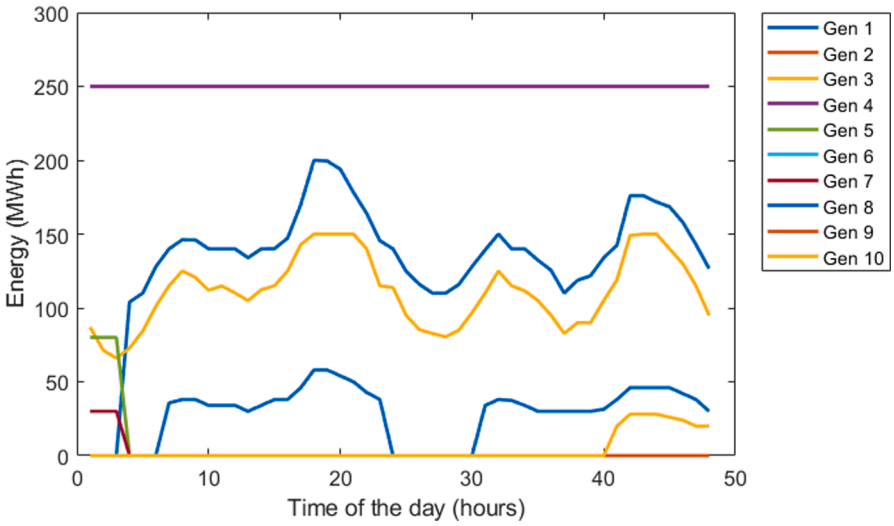

Fig. 3. Hourly energy supplied by generating units.

beginning of the scheduling horizon. Therefore, generator 4, which has the lowest operating cost, remains operational the entire time while more expensive generators such as generators 5 and 7 are shut down for the rest of time. The optimal total cost of power generation in this case is $420,079.1. As shown in Fig. 4, the system in the base case does not consider load leveling and there is no evidence of peak shaving.

3.2. Case 2–4 UC problem with PEV charging only

When PEVs are incorporated into the system, the generators carry out unit commitment to minimize the cost of power generation for supplying both the PEV loads and non-PEV loads. Fig. 5 (a-c) shows the hourly PEV and non-PEV demand and the total power generated during the day for each penetration level. The introduction of PEVs in the system in a charging only case causes significant increase in peak load and total generated power especially at higher penetration levels. This can be seen clearly in the case of 1,000,000 PEVs in Fig. 5c, where the energy demand of PEVs significantly exceeds the non-PEV demand. The additional load of PEVs is significantly higher than non-PEV load during the peak hours and causes sharp increase in power generation.

Fig. 6a-c shows the behavior of the generating units during the analysis period. Unsurprisingly, as the number of PEVs in the system increases, more generators come online to address this additional load. As can be seen from the results, charging patterns of 10,000 PEVs have minimal impact on total non-PEV load demand and the behavior of the generating units when compared to the base case. However, at higher penetration levels PEVs have significant impact on the system as can be seen in Fig. 5b and 5c. This results in more units being committed during the day. In the case of one million PEVs, there is an additional ramp-up of generator 4 to satisfy the sharp increase in demand.

In all cases, generator 4 which has the lowest operating cost operates during the entire period compared to other generators such as generators 2, 6, and 9 that have high operating costs and therefore remain mostly in a shutdown state to minimize the cost of generation in the first two cases while remaining within their power capacity constraints. At the highest level of penetration, all generators are committed during the peak hours between hours 7 and 23 as shown in Fig. 6c. The total cost of power generation with unidirectional PEV charging is $422,029, $439,133, and $627,949 for 10,000, 100,000 and 1,000,000 PEVs, respectively.

3.3. Case 5–7 UC problem with PEVs and V2G

When V2G is incorporated into the UC model, PEV batteries act as

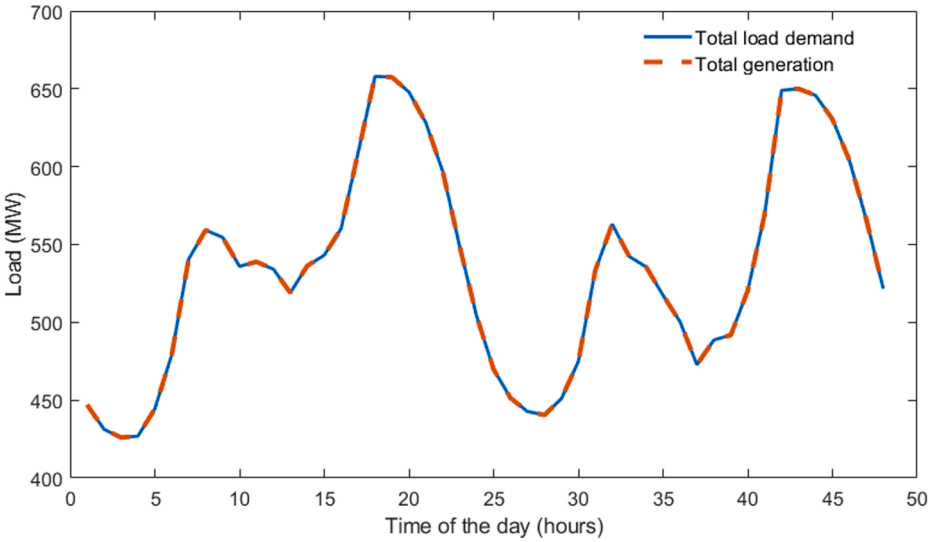

Fig. 4. Hourly generation and load demand.

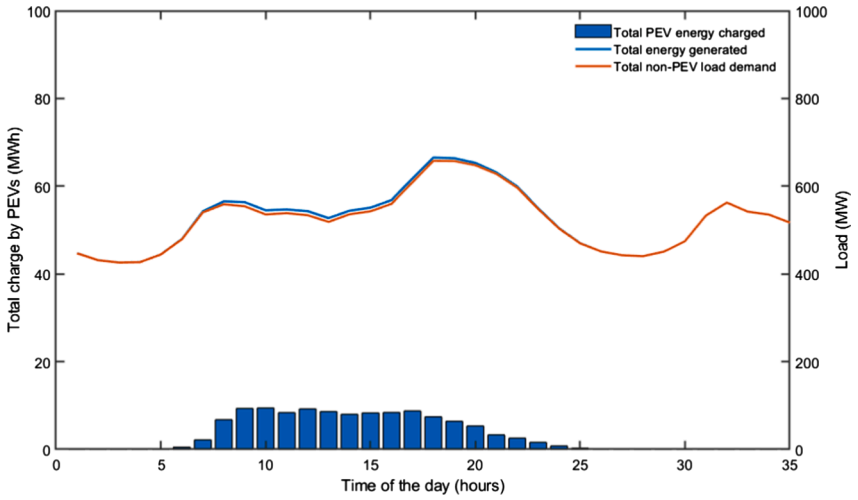

a) 10,000 PEVs

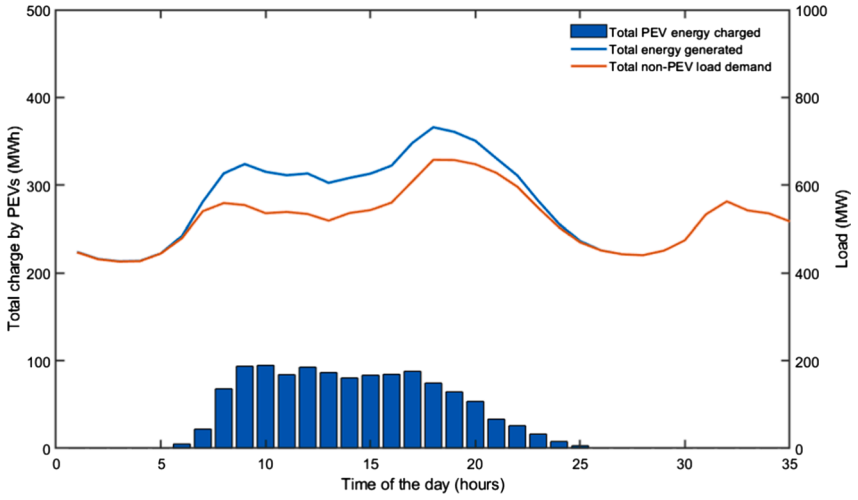

b) 100,000 PEVs

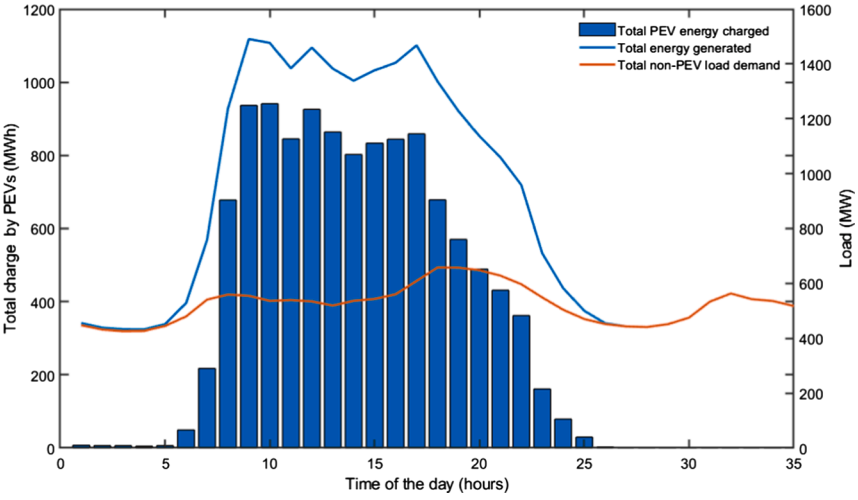

c) 1,000,000 PEVs

Fig. 5. Hourly power generation and load demand with PEV charging only.

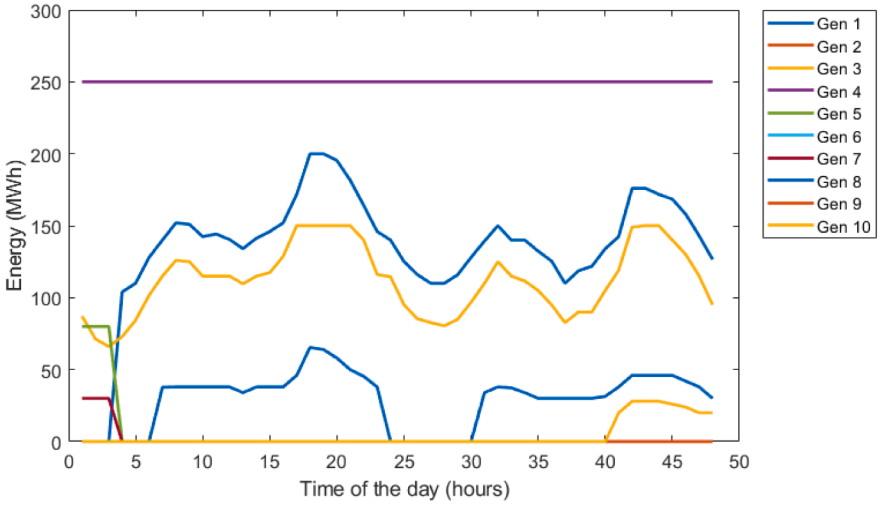

a) 10,000 PEVs

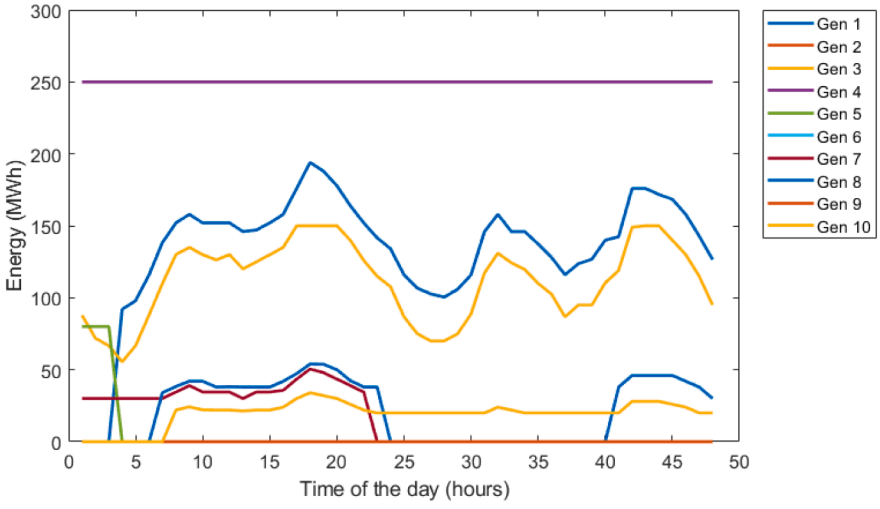

b) 100,000 PEVs

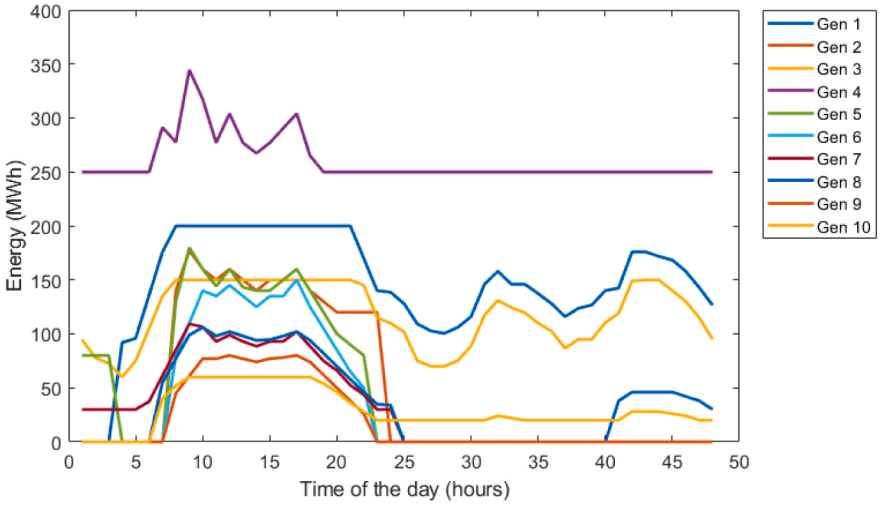

c) 1,000,000 PEVs

Fig. 6. Hourly energy supplied by generating units in charging only cases.

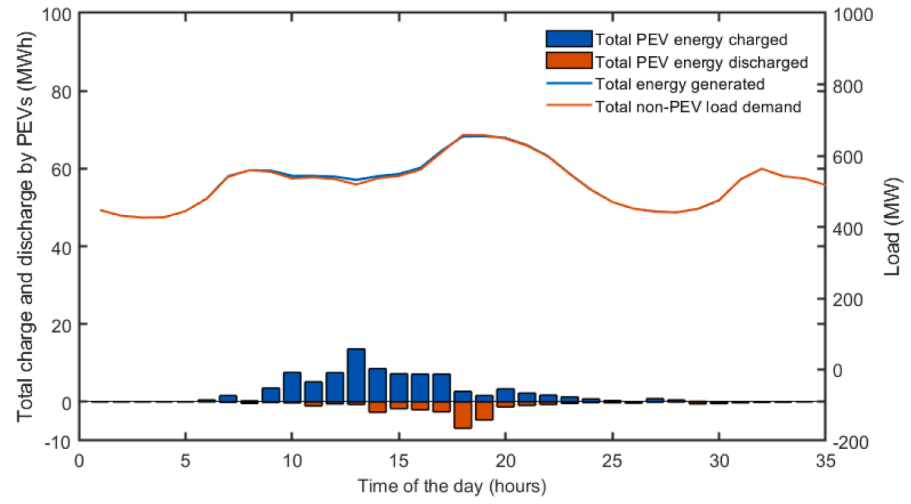

a) 10,000 PEVs

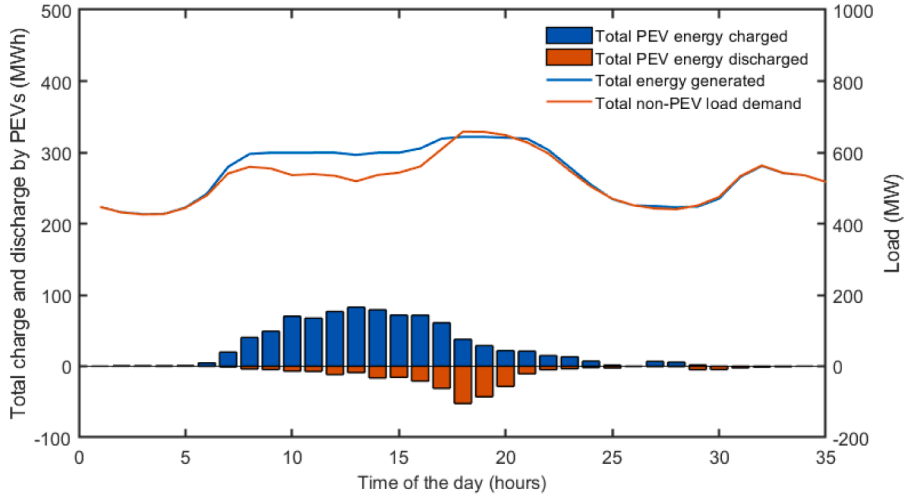

b) 100,000 PEVs

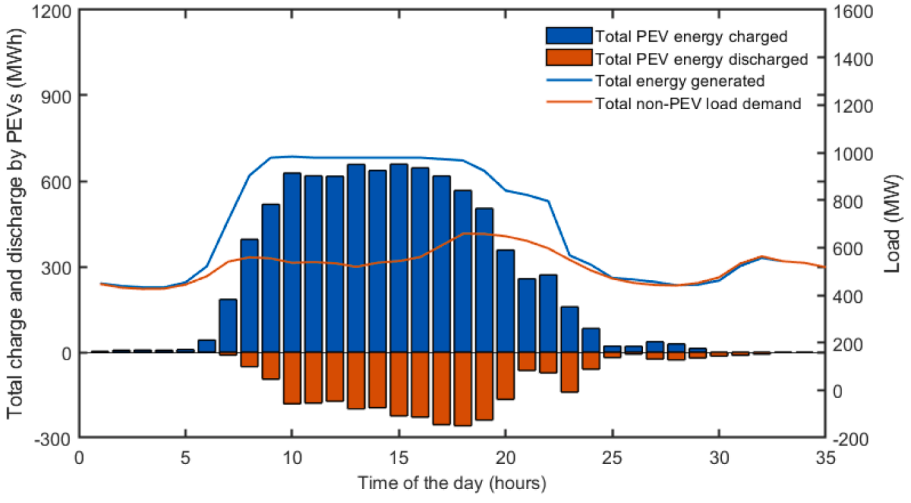

c) 1,000,000 PEVs

Fig. 7. Hourly power generation and load demand for V2G cases.

energy storage in the system to support the generators during peak hours by discharging. Fig. 7a-c shows the power demand and supply of the system with V2G implemented at each penetration level. A closer look at the total power generated curve, and the total non-PEV load demand curve shows that minimal peak shaving occurs between hours 18 and 19 with 10,000 PEVs. Significant load leveling can be observed at higher

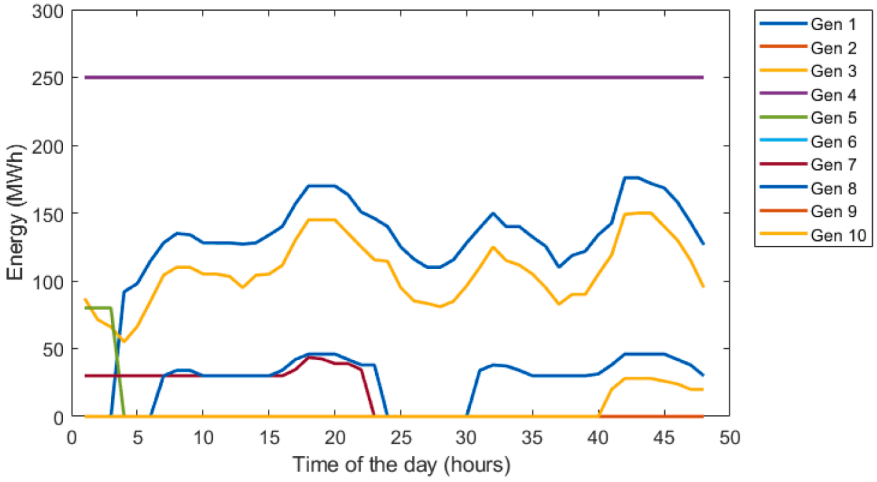

a) 10,000 PEVs

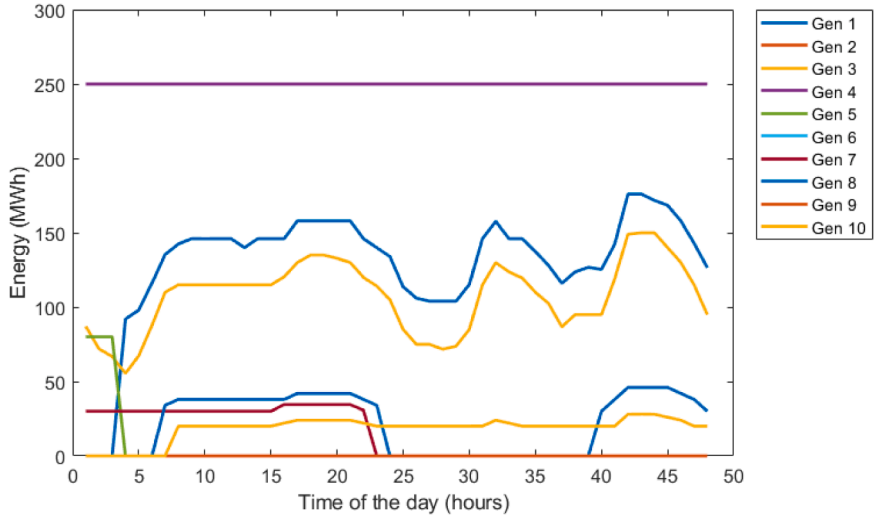

b) 100,000 PEVs

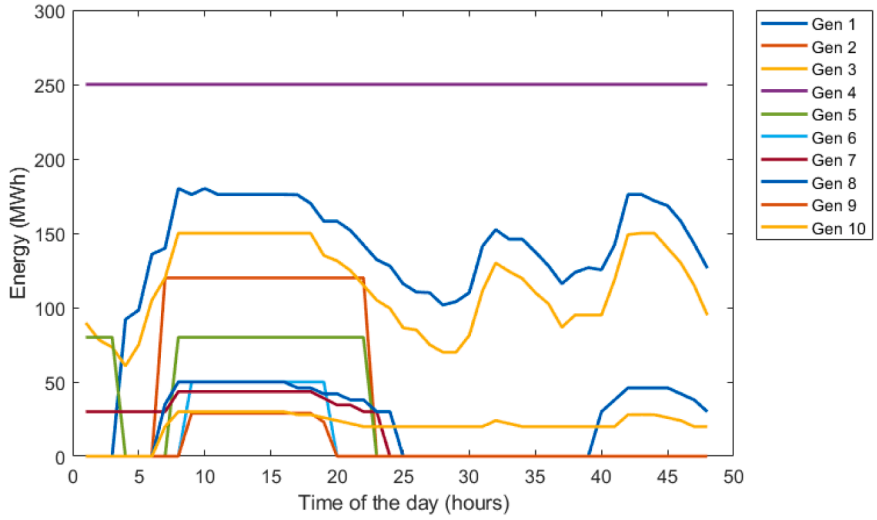

c) 1,000,000 PEVs

Fig. 8. Hourly energy supplied by generating units in V2G cases.

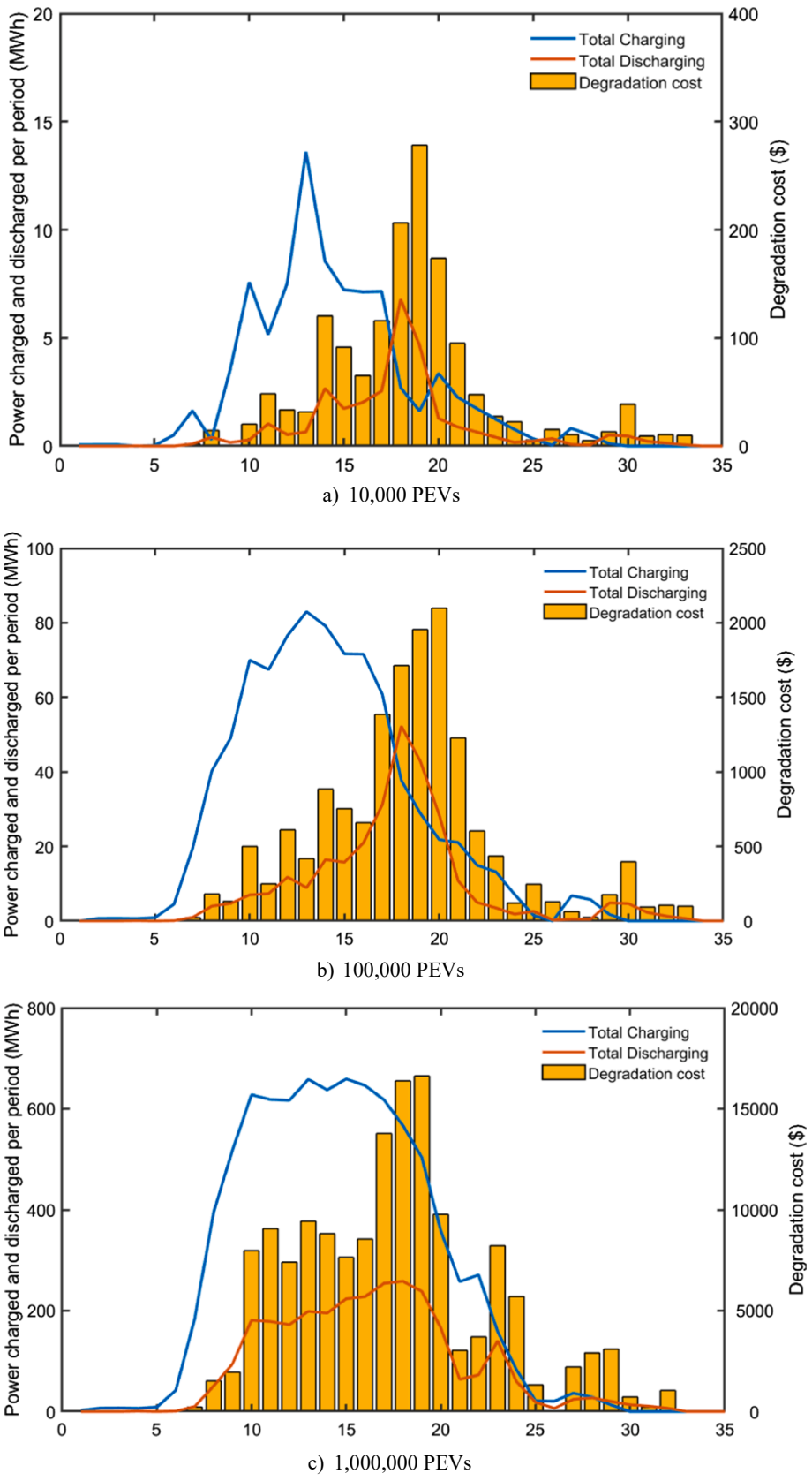

Fig. 9. Hourly battery degradation cost.

penetration levels. As can be observed, V2G implementation plays a significant role in load leveling to support the grid during periods of high load demand.

The unit commitment behavior of the generators in the V2G case are shown in Fig. 8a-c. The impact of V2G can be observed in flattening the generators profiles during the peak hours particularly in the system with

Table 2
Results of different penetration levels.

Case	Total generation cost (USD)	Degradation cost (USD)	Average Cost per unit energy ($/MWh)
Base Case (no PEVs)	420,079	0	16.372
10,000 PEVs (charging only)	422,029	0	16.374
10,000 PEVs (V2G)	420,875	1,513	16.367
100,000 PEVs (charging only)	439,133	0	16.372
100,000 PEVs (V2G)	429,120	15,123	16.364
1,000,000 PEVs (charging only)	627,949	0	16.839
1,000,000 PEVs (V2G)	514,407	151,453	16.426

1,000,000 PEVs. as shown in Fig. 8a-c. At the highest level of PEV penetration, all generators are committed during the peak hours while V2G is providing additional capacity to the system. The additional capacity keeps the generation units operating at constant power level, reduces ramping-up or avoids the cost of starting-up another generator to satisfy the demand. The total cost of power generation by the thermal units in a system with V2G is $420,875, $429,120, and $514,407 for 10,000, 100,000 and 1,000,000 PEVs, respectively.

Fig. 9 illustrates the hourly cost of battery degradation of PEVs participating in the system at each penetration level. The degradation cost considers the cost of the battery and the amount of cycling that takes place during V2G. Therefore, an increase in the degradation cost is seen in periods where there is a high discharging frequency. The total cost of battery degradation for 10,000, 100,000 and 1,000,000 vehicles are $1,513, $15,123, and $151,453, respectively.

3.4. Comparative analysis

Implementing the model successfully reduces the total cost of power generation by the thermal units at each of the three penetration levels when comparing V2G to the charging only scenario. An additional 566 MWh is introduced from the deployment of 100,000 PEVs with V2G compared with the base case, and the peak load is reduced by 7.9 MWh due to load leveling. In comparison, the charging only scenario adds 1163 MWh and increases the peak load by 74.5 MWh. With a million PEVs in the system, the difference between the two scenarios in peak load values is 512.5 MW or 34% reduction in peak load due to the implementation of V2G. This significant load leveling and reduction in power generation comes with additional battery degradation cost due to discharging as presented in Table 2. However, this additional cost is offset by reduction in power generation and by load leveling.

According to Table 2, the use of V2G for controlled charging and discharging in this study reduced the total cost of power generation when compared to the charging only cases by 0.3%, 2.3% and 18.1% for 10,000, 100,000, and 1,000,000 vehicles, respectively. Furthermore, the three cases involving V2G maintained a lower average cost per unit energy compared to the charging only cases with a maximum decrease of 0.41 $/MWh at the highest level of penetration. The average cost per unit energy in Table 2 is defined as the total cost of generation divided by the total power produced by the 10 generators. Therefore, this value does not consider the battery degradation cost. Considering battery degradation cost increases the average cost per unit energy (in $/MWh) in the V2G cases to 16.426 $/MWh, 16.940 $/MWh, and 21.263 $/MWh for 10,000, 100,000 and 1,000,000 vehicles respectively.

Fig. 10 shows a comparison of the cost per unit energy values between the cases that involve PEV charging only and cases with V2G over a range of penetration levels. A small improvement of 0.01 $/MWh in cost per unit energy can be observed in the case of 100,000 vehicles with V2G when compared to the charging only case, however significant improvement of 0.41$/MWh can be observed with 1,000,000 vehicles. In all cases, incorporating V2G results in lower total generation costs compared to charging only scenarios. Fig. 10 shows that in all but 2 cases

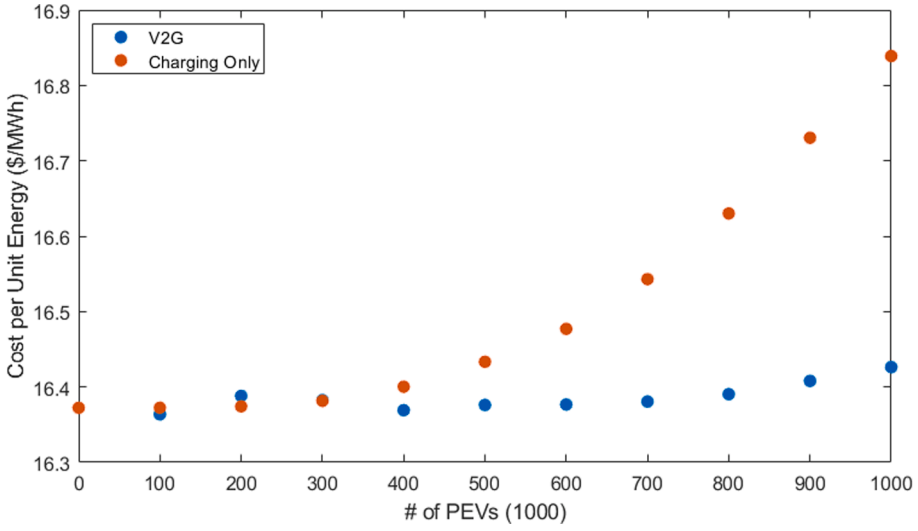

Fig. 10. Comparison of average cost per unit energy for different PEV penetration levels.

(200,000 and 300,000 PEV cases), the V2G option outperforms the charging only cases in terms of average cost per unit energy. In those two cases, the differences in cost per unit energy between the V2G and charging only scenarios are 0.084% and 0.006% for 200,000 and 300,000 PEVs respectively. The average cost per unit energy in Fig. 10 does not consider the cost of battery degradation. The cost of degradation when considered at the different penetration levels has a significant impact on the economic feasibility of V2G for solving unit commitment. Increasing the number of vehicles participating in V2G resulted in an increase in battery degradation costs due to increased cycling of vehicle batteries. The highest level of penetration with V2G incurs a total battery degradation cost of $151,453. Our results show clear evidence of load leveling in V2G cases, especially at higher penetration levels. These findings are similar to those in the literature [16,26,17] confirming that load leveling is a clear benefit of implementing V2G which can be utilized as an ancillary service to reduce the risk of line congestions in the system. By delaying charging of PEVs to periods of lesser congestions or power demand, V2G can result in valley filling and peak shaving of the power profile as shown in Fig. 7a-c.

Similar studies have been selected from the literature for comparison as shown in Table 3. The majority of the reviewed studies formulated the UC problem as MILP or MINLP problems with DC power flow equations. Different numbers of PEVs have been considered ranging between 10,000 and 250,000 vehicles. In Yang et al. [21], incorporating V2G into the UC problem with 50,000 PEVs reduced the total generation cost by 2.04% when compared to the charging only case. In our study, the V2G mode resulted in total generation cost that was 2.28% lower than the charging only mode when 100,000 PEVs are considered. When compared to the base case, our results show an increase of 2.15% (with 100,000 PEVs) in total generation cost due to the introduction of PEVs in the system as an additional load when V2G is implemented. Zhu et al. [49], reported 2.72% increase in total generation cost with 150,000 PEVs and Yang et al. [26] reported 0.29% increase with 50,000 PEVs. Based on our findings, there is a 22.45% increase in generation cost compared to the base case when the penetration level increases to 1,000,000 PEVs as can be seen in Table 3. Similar results have been reported by Madzharov et al. [52], where the authors concluded that the generation cost increases by 1% for every 10% increase in PEV penetration. Vasiyullah and Bharathidasan [27] presented a nonlinear profit-based UC model with renewable sources and 50,000 PEVs and reported 4.91% increase in generation cost due to the introduction of PEVs.

Several of the reviewed studies reported a reduction in total cost when compared to the base case due to including the cost of V2G operation in the objective function as in [34,22,51,47,19,24], emission costs as in [48], assuming that all PEVs obtain their energy requirement from renewable energy sources as in [21,26], or considering spinning reserve as in [50,16,25]. None of the reviewed models included the cost of battery degradation which is a significant cost especially at high penetration levels as our results show in Table 2. When the cost of battery degradation is considered, the total cost for the V2G cases compared to the base case increases by 5.75% and 58.51% for 100,000 and 1,000,000 PEVs respectively.

4. Conclusion

In this paper, a unit commitment problem with controlled V2G framework was developed to study the impact of high penetration levels of PEVs on the grid. A robust driving and charging/discharging behavior pattern method is used to generate different scenarios from historical data. In addition, battery degradation due to cycling from charging/discharging is considered. The economic impact of multiple cases with different penetration levels are evaluated with and without V2G. The results reveal that in all cases, the management of PEV charging and discharging reduces the total cost of power generation when compared to the charging only scenario. In all but two of the ten levels of PEV penetration evaluated, the V2G scenario reduces the average cost per unit energy compared to the charging only scenario. In both cases where the average cost per unit energy is higher for the V2G setup, the difference is very small (0.084% and 0.006%) and lower total generation cost is realized with V2G compared to the charging only cases. Although the use of V2G does not result in a significant reduction in cost per unit energy when compared to the base case, the proposed model has successfully maintained the cost per unit energy at the same level with minimal increase, despite the quadratic energy generation cost (see Equation (1)). The cost of degradation, when considered at the different penetration levels, has a significant impact on the economic feasibility of V2G. PEVs in the system contribute to load leveling which is desirable for power systems. This ancillary service can be very useful in systems that are prone to congestions or overloading. At the highest level of penetration, the model in this study shows that controlled V2G operation is capable of significantly reducing the total generation cost by 18.08% compared to the charging only case. Load leveling during peak

Table 3
A comparison of the proposed model with existing literature.

Reference	UC Formulation	Deterministic / Stochastic	#PEVs (1000)	Cost of generation ($)		Difference (%)
				Without PEVs	With V2G	
[21]	MINLP	Deterministic	50	563,937	556,343	1.35%
[22]	MILP	Deterministic	10	136,335	134,345	1.46%
[24]	MINLP	Deterministic	40	563,839	554,451	1.67%
[19]	MILP	Deterministic	10	162,423	157,239	3.19%
[34]	MILP	Deterministic	10	136,335	114,975	15.67%
[16]	MILP	Stochastic	10	119,261	105,331	11.68%
[25]	MINLP	Stochastic	50	563,979	561,665	0.41%
[47]	MILP	Deterministic	10	117,180	112,360	4.11%
[48]	MILP	Stochastic	25	556,118	542,592	2.43%
[26]	MINLP	Deterministic	50	563,937	565,572	−0.29%
[49]	MINLP	Deterministic	150	563,937	579,255	−2.72%
[50]	MINLP	Stochastic	50	719,152	677,188	5.84%
[51]	MINLP	Deterministic	240	564,714	557,554	1.27%
[27]	MINLP	Deterministic	50	533,187	559,367	−4.91%
Proposed Model	MILP	Deterministic	100	420,079	429,120	−2.15
			1000	420,079	514, 407	−22.45%

hours can be observed in all cases which results in reduction of peak load and steady operating levels for generators. This is significant to reduce ramping-up or starting up additional units for a short amount of time to satisfy any sudden increase in demand.

The effect of single-phase car chargers on grid operation is outside the scope of this paper. The solution proposed in this study assumes a commercial charging station serving a large number of vehicles. Such a commercial facility would use well-known three phase balancing techniques, including active load balancers. A possible extension to this work involves considering a simulation with a larger unbalanced system. The authors anticipate that considering a larger unbalanced system will result in power losses and an increase in total generation cost. Another extension to this study is the consideration of renewable energy resources in the UC problem. PEV batteries can be useful as a reservoir to store renewable energy during periods of excess generation for use in periods when the renewable energy is not operational. Furthermore, future work can analyze emissions cost from the use of thermal generators. This will require the emissions data of the specific generators used in the system. Emissions and cost objectives that might be conflicting can be accounted for as multi-objective scenarios.

CRediT authorship contribution statement

Ona Egbue: Conceptualization, Methodology, Formal analysis, Writing – original draft, Writing – review & editing, Supervision, Project administration. **Charles Uko:** Methodology, Formal analysis. **Ali Aldubaisi:** Formal analysis, Writing – original draft, Writing – review & editing. **Enrico Santi:** Writing – review & editing, Supervision.

Declaration of Competing Interest

The authors declare that they have no known competing financial interests or personal relationships that could have appeared to influence the work reported in this paper.

Acknowledgements

This work was partially funded by the National Science Foundation award #1711767.

References

[1] The Paris Agreement. Paris agreement. Report of the Conference of the Parties to the United Nations Framework Convention on Climate Change (21st Session, 2015: Paris); 2015.
[2] Hockstad, L., Hanel, L., 2018. Inventory of U.S. Greenhouse Gas Emissions and Sinks. https://doi.org/10.15485/1464240.
[3] Ascher D, Hackenberg G. Integrated transportation and power system modeling. 2015 International Conference on Connected Vehicles and Expo (ICCVE). 2015.
[4] Ding Z, Lu Y, Lai K, Yang M, Lee W-J. Optimal coordinated operation scheduling for electric vehicle aggregator and charging stations in an integrated electricity-transportation system. Int J Electr Power Energy Syst 2020;121:106040. https://doi.org/10.1016/j.ijepes.2020.106040.
[5] Mortaz E, Valenzuela J. Microgrid energy scheduling using storage from electric vehicles. Electr Power Syst Res 2017;143:554–62. https://doi.org/10.1016/j.epsr.2016.10.062.
[6] Ramakrishna Reddy K, Meikandasivam S, Vijayakumar D. A novel strategy for maximization of plug-In electric vehicle's storage utilization for grid support with consideration of customer flexibility. Electr Power Syst Res 2019;170:158–75. https://doi.org/10.1016/j.epsr.2018.12.031.
[7] Sami I, Ullah Z, Salman K, Hussain I, Ali SM, Khan B, Mehmood CA, Farid, U, 2019. A bidirectional interactive electric vehicles operation modes: vehicle-to-grid (V2G) and grid-to-vehicle (G2V) variations within smart grid. 2019 International Conference on Engineering and Emerging Technologies (ICEET).
[8] Kisacikoglu MC, Ozpineci B, Tolbert LM. EV/PHEV bidirectional charger assessment for V2G reactive power operation. IEEE Trans Power Electron 2013;28(12):5717–27. https://doi.org/10.1109/TPEL.2013.2251007.
[9] Tan KM, Ramachandaramurthy VK, Yong JY. 2016/01/01/). Integration of electric vehicles in smart grid: a review on vehicle to grid technologies and optimization techniques. Renew Sustain Energy Rev 2016;53:720–32. https://doi.org/10.1016/j.rser.2015.09.012.
[10] Putz D, Schwabeneder D, Auer H, Fina B. A comparison between mixed-integer linear programming and dynamic programming with state prediction as novelty for solving unit commitment. Int J Electr Power Energy Syst 2021;125:106426. https://doi.org/10.1016/j.ijepes.2020.106426.
[11] Abdi H. Profit-based unit commitment problem: a review of models, methods, challenges, and future directions. Renew Sustain Energy Rev 2021;138:110504. https://doi.org/10.1016/j.rser.2020.110504.
[12] Håberg M. Fundamentals and recent developments in stochastic unit commitment. Int J Electr Power Energy Syst 2019;109:38–48. https://doi.org/10.1016/j.ijepes.2019.01.037.
[13] Kërçi T, Giraldo J, Milano F. Analysis of the impact of sub-hourly unit commitment on power system dynamics. Int J Electr Power Energy Syst 2020;119:105819. https://doi.org/10.1016/j.ijepes.2020.105819.
[14] Howlader HOR, Matayoshi H, Noorzad AS, Muarapaz CC, Senjyu T. Smart house-based optimal operation of thermal unit commitment for a smart grid considering transmission constraints. Int J Sustain Energ 2018;37(5):438–54. https://doi.org/10.1080/14786451.2017.1284849.
[15] Khodayar ME, Wu L, Shahidehpour M. Hourly coordination of electric vehicle operation and volatile wind power generation in SCUC. IEEE Trans Smart Grid 2012;3(3):1271–9. https://doi.org/10.1109/TSG.2012.2186642.
[16] Rahmani M, Hosseinian SH, Abedi M. Stochastic two-stage reliability-based security constrained unit commitment in smart grid environment. Sustainable Energy Grids Networks 2020;22:100348. https://doi.org/10.1016/j.segan.2020.100348.
[17] Yoshioka N, Asano H, Bando S. Economic evaluation of charging/discharging control of electric vehicles as system flexibility considering control participation rate. Electr Eng Jpn 2020;211(1–4):15–25. https://doi.org/10.1002/eej.23267.
[18] Park H, Jin YG, Park J-K. Stochastic security-constrained unit commitment with wind power generation based on dynamic line rating. Int J Electr Power Energy Syst 2018;102:211–22. https://doi.org/10.1016/j.ijepes.2018.04.026.
[19] Hosseini Imani M, Jabbari Ghadi M, Shamshirband S, Balas MM. Impact evaluation of electric vehicle parking on solving security-constrained unit commitment problem. Math Computat Appl 2018;23(1):13. https://www.mdpi.com/2297-8747/23/1/13.
[20] Sadeghian H, Wang Z, 2017. Combined heat and power unit commitment with smart parking lots of plug-in electric vehicles. 2017 North American Power Symposium (NAPS).
[21] Yang Z, Li K, Guo Y, Feng S, Niu Q, Xue Y, et al. A binary symmetric based hybrid meta-heuristic method for solving mixed integer unit commitment problem integrating with significant plug-in electric vehicles. Energy 2019;170:889–905. https://doi.org/10.1016/j.energy.2018.12.165.
[22] Azari AN, Soleymani S, Mozafari B, Sarfi G. Optimal transmission congestion management with V2G in smart grid. Am J Electr Power Energy Syst 2018;7(2):16–24.
[23] Cao H, Zhao Q. A Novel Game-Theoretic-based Security-Constrained Unit Commitment Including Wind and Vehicle-to-Grid. 2019 Chinese Control And Decision Conference (CCDC). 2019.
[24] Maghsudlu S, Mohammadi S. Optimal scheduled unit commitment considering suitable power of electric vehicle and photovoltaic uncertainty. J Renew Sustain Energy 2018;10(4):043705. https://doi.org/10.1063/1.5009247.
[25] Shahbazitabar M, Abdi H. A novel priority-based stochastic unit commitment considering renewable energy sources and parking lot cooperation. Energy 2018;161:308–24. https://doi.org/10.1016/j.energy.2018.07.025.
[26] Yang Z, Li K, Niu Q, Xue Y. A comprehensive study of economic unit commitment of power systems integrating various renewable generations and plug-in electric vehicles. Energy Convers Manage 2017;132:460–81. https://doi.org/10.1016/j.enconman.2016.11.050.
[27] Vasiyullah SFS, Bharathidasan SG. Profit based unit commitment of thermal units with renewable energy and electric vehicles in power market. J Electr Eng Technol 2021;16(1):115–29. https://doi.org/10.1007/s42835-020-00579-3.
[28] Marmaras C, Xydas E, Cipcigan L. Simulation of electric vehicle driver behaviour in road transport and electric power networks. Transport Res C: Emerg Technol 2017;80:239–56. https://doi.org/10.1016/j.trc.2017.05.004.
[29] Uko C, Egbue O, Naidu DS. Economic dispatch of a smart grid with vehicle-to-grid integration. 2020 IEEE Green Technologies Conference(GreenTech), Oklahoma City, OK; 2020.
[30] Shamshirband M, Salehi J, Samadi Gazijahani F. 2019/08/01/). Look-ahead risk-averse power scheduling of heterogeneous electric vehicles aggregations enabling V2G and G2V systems based on information gap decision theory. Electr Power Syst Res 2019;173:56–70. https://doi.org/10.1016/j.epsr.2019.04.018.
[31] Deng R, Xiang Y, Huo Da, Liu Y, Huang Y, Huang C, et al. Exploring flexibility of electric vehicle aggregators as energy reserve. Electr Power Syst Res 2020;184:106305. https://doi.org/10.1016/j.epsr.2020.106305.
[32] Pan A, Ge X, Wang Y, Pei C, Xia S, 2019. Stochastic Security Constraint Unit Commitment Considering the Correlation of Electric Vehicles' Driving. 2019 IEEE Innovative Smart Grid Technologies - Asia (ISGT Asia).
[33] Ahrabi M, Abedi M, Nafisi H, Mirzaei MA, Mohammadi-Ivatloo B, Marzband M. Evaluating the effect of electric vehicle parking lots in transmission-constrained AC unit commitment under a hybrid IGDT-stochastic approach. Int J Electr Power Energy Syst 2021;125:106546. https://doi.org/10.1016/j.ijepes.2020.106546.
[34] Ahmadi A, Esmaeel Nezhad A, Siano P, Hredzak B, Saha S. Information-gap decision theory for robust security-constrained unit commitment of joint renewable energy and gridable vehicles. IEEE Trans Ind Inf 2020;16(5):3064–75. https://doi.org/10.1109/TII.2019.2908834.
[35] Uko C. Optimization of Vehicle to Grid System in a Power System with Unit Commitment [Master's Thesis, University of South Carolina]; 2020. https://scholarcommons.sc.edu/etd/5964.

[36] Teyabeen AA, Akkari FR, Jwaid AE. 5–7 April). Power Curve Modelling for Wind Turbines. 2017 UKSim-AMSS 19th International Conference on Computer Modelling Simulation (UKSim). 2017.
[37] Department of Energy. (2018). *Fuel Economy Data* https://www.fueleconomy.gov/feg/download.shtml.
[38] George-Williams H, Patelli E. Maintenance strategy optimization for complex power systems susceptible to maintenance delays and operational dynamics. IEEE Trans Reliab 2017;66(4):1309–30.
[39] Liang H, Liu Y, Li F, Shen Y. Dynamic economic/emission dispatch including PEVs for peak shaving and valley filling. IEEE Trans Ind Electron 2019;66(4):2880–90.
[40] Soroudi A. Power Syst Optim Model GAMS 2017;78:Springer. https://doi.org/10.1007/978-3-319-62350-4.
[41] Saldaña G, San Martin JI, Zamora I, Asensio FJ, Oñederra O. Electric vehicle into the grid: charging methodologies aimed at providing ancillary services considering battery degradation. Energies 2019;12(12):2443. https://www.mdpi.com/1996-1073/12/12/2443.
[42] Liu K, Chen Q, Kang C, Su W, Zhong G. Optimal operation strategy for distributed battery aggregator providing energy and ancillary services. J Mod Power Syst Clean Energy 2018;6(4):722–32. https://doi.org/10.1007/s40565-017-0325-9.
[43] Ortega-Vazquez MA. Optimal scheduling of electric vehicle charging and vehicle-to-grid services at household level including battery degradation and price uncertainty [https://doi.org/10.1049/iet-gtd.2013.0624]. IET Gener Transm Distrib 2014;8(6):1007-1016. https://doi.org/10.1049/iet-gtd.2013.0624.
[44] Coffin D, Horowitz J. The supply chain for electric vehicle batteries. J Int Commerce Econ 2018;1.
[45] Irle R. Global EV Sales for the 1st Half of 2019; 2019. http://www.ev-volumes.com/country/total-world-plug-in-vehicle-volumes/.
[46] GAMS, 2020. GAMS Documentation 33: CPLEX 12 Retrieved 09/20/2021 from https://www.gams.com/33/docs/S_CPLEX.html.
[47] Haddadian G, Khalili N, Khodayar M, Shahiedehpour M. Security-constrained power generation scheduling with thermal generating units, variable energy resources, and electric vehicle storage for V2G deployment. Int J Electr Power Energy Syst 2015;73:498–507. https://doi.org/10.1016/j.ijepes.2015.05.020.
[48] Soltani Z, Ghaljehei M, Gharehpetian GB, Aalami HA. Integration of smart grid technologies in stochastic multi-objective unit commitment: an economic emission analysis. Int J Electr Power Energy Syst 2018;100:565–90. https://doi.org/10.1016/j.ijepes.2018.02.028.
[49] Zhu X, Zhao S, Yang Z, Zhang N, Xu X. A parallel meta-heuristic method for solving large scale unit commitment considering the integration of new energy sectors. Energy 2022;238:121829. https://doi.org/10.1016/j.energy.2021.121829.
[50] Gupta PP, Jain P, Sharma KC, Bhaker R. Optimal scheduling of electric vehicle in stochastic AC SCUC problem for large-scale wind power penetration [https://doi.org/10.1002/2050-7038.12145]. Int Trans Electr Energy Syst 2020;30(4):e12145. https://doi.org/10.1002/2050-7038.12145.
[51] Bioki MMH, Jahromi MZ, Rashidinejad M. A combinatorial artificial intelligence real-time solution to the unit commitment problem incorporating V2G. Electr Eng 2013;95(4):341–55. https://doi.org/10.1007/s00202-012-0263-5.
[52] Madzharov D, Delarue E, D'Haeseleer W. Integrating electric vehicles as flexible load in unit commitment modeling. Energy 2014;65:285–94. https://doi.org/10.1016/j.energy.2013.12.009.